CHAPTER THIRTY-TWO

Voltage-Clamp-Based Methods for the Detection of Constitutively Active Acetylcholine-Gated $I_{K,ACh}$ Channels in the Diseased Heart

Niels Voigt,* Samy Makary,† Stanley Nattel,† *and* Dobromir Dobrev*

Contents

Abstract

Vagal nerve stimulation can promote atrial fibrillation (AF) that requires activation of the acetylcholine (ACh)-gated potassium current $I_{K,ACh}$. In chronic AF (cAF), $I_{K,ACh}$ shows strong activity despite the absence of ACh or analogous pharmacological stimulation. This receptor-independent, constitutive $I_{K,ACh}$ activity is suggested to represent an atrial-selective anti-AF therapeutic target, but the underlying molecular mechanisms are unknown. This chapter provides an overview of the voltage-clamp techniques that can be used to study

* Division of Experimental Cardiology, Department of Internal Medicine I—Cardiology, Angiology, Pneumology, Intensive Care and Hemostaseology, Medical Faculty Mannheim, University of Heidelberg, Theodor-Kutzer-Ufer, Mannheim, Germany
† Research Center, Montreal Heart Institute, Montreal, Quebec, Canada

Methods in Enzymology, Volume 484
ISSN 0076-6879, DOI: 10.1016/S0076-6879(10)84032-7

constitutive $I_{K,ACh}$ activity in atrial myocytes and summarizes briefly the current knowledge about the potential underlying mechanism(s) of constitutive $I_{K,ACh}$ activity in diseased heart.

1. Introduction

Stimulation of the vagal nerve decelerates the heart rate due to release of acetylcholine (ACh). This was demonstrated for the first time by Otto Loewi in 1921 and the "Vagusstoff" (ACh) became the first neurotransmitter ever discovered (Loewi, 1921). However, it took more than 50 years until it was suggested that ACh activates a specific population of K^+ channels (ACh-gated $I_{K,ACh}$) leading to hyperpolarization of the cell membrane thereby decreasing pacemaker activity in sinoatrial node cells (Noma and Trautwein, 1978). In 1983, Sakmann *et al.* recorded single-channel openings of $I_{K,ACh}$ in rabbit atrial and sinus node cells and showed that $I_{K,ACh}$ channels exhibit kinetic properties clearly different from those of the background inwardly rectifying K^+ channel I_{K1} (Sakmann *et al.*, 1983). Cardiac $I_{K,ACh}$ channels were identified as heterotetramers consisting of two Kir3.1 and two Kir3.4 channel subunits (Krapivinsky *et al.*, 1995).

Today, it is well known that ACh binding to type 2 muscarinic receptors (M_2 receptors) leads to dissociation of inhibitory G_i proteins and to activation of $I_{K,ACh}$ due to direct interaction of G protein $\beta\gamma$-subunits with the channel (for review, see Hibino *et al.*, 2010; Yamada *et al.*, 1998). Apart from the canonical M_2-receptor-mediated activation of $I_{K,ACh}$, purinergic A_1 (Dobrev *et al.*, 2000; Kurachi *et al.*, 1986) and sphingolipid Edg-3 (Himmel *et al.*, 2000) receptors, coupled to G_i proteins as well, can also activate cardiac $I_{K,ACh}$ channels. Taking account of this heterologous regulation, $I_{K,ACh}$ channels are also designated as G protein-activated inwardly rectifying K^+ channels (GIRK channels). In neurons and various endocrine cells, GIRK channels are also activated by neurotransmitters that target α_2-adrenoceptors, opioid (μ, δ, and κ), D_2 dopamine, $GABA_B$, m-Glu, 5-hydroxytryptamine-1A, and somatostatin receptors, thereby contributing to formation of slow inhibitory postsynaptic potentials and inhibition of hormone release (for review, see Hibino *et al.*, 2010; Yamada *et al.*, 1998). Because of strong activation of GIRK channels by neurotransmitters, tonic (constitutive) $I_{K,ACh}$ activity in the absence of receptor agonists is often regarded as negligible. However, it was early recognized that $I_{K,ACh}$ possesses an agonist-independent "resting" activity, which occurred with a much lower opening frequency (Sakmann *et al.*, 1983). Physiologically constitutive $I_{K,ACh}$ channels may underlie a major part of basal K^+ conductance in sinoatrial cells which lack I_{K1}, playing an important role in regulating heart rate (Ito *et al.*, 1994). In addition, constitutively active GIRK

channels have been shown to contribute to the resting membrane potential of murine hippocampal pyramidal cells (Luscher *et al.*, 1997) and rat locus coeruleus slices (Blanchet and Luscher, 2002).

In normal heart constitutive $I_{K,ACh}$ activity is very low but may increase substantially during cardiac diseases. For instance, agonist-independent constitutive $I_{K,ACh}$ activity increases in atrial myocytes from patients with chronic atrial fibrillation (cAF) and dogs with atrial tachycardia-induced remodeling (ATR; Cha *et al.*, 2006; Dobrev *et al.*, 2005; Voigt *et al.*, 2008). Constitutive $I_{K,ACh}$ channels may contribute to the shortening of the atrial action potential duration (APD), which is a hallmark of the AF-associated changes in atrial electrical properties (electrical remodeling; Dobrev, 2006; Nattel *et al.*, 2008). *In vivo*, vagal nerve stimulation abbreviates APD, increases APD heterogeneity, and enhances atrial vulnerability to tachyarrhythmias, which induce and perpetuate AF (Liu and Nattel, 1997). In knockout mice lacking the Kir3.4 channel subunit, M-receptor stimulation did not induce AF, clearly suggesting that the effects of vagal nerve activation are exclusively mediated by $I_{K,ACh}$ (Kovoor *et al.*, 2001). Thus, agonist-independent constitutive $I_{K,ACh}$ channels during cAF are expected to increase atrial vulnerability to tachyarrhythmias and to promote persistence of AF. Accordingly, inhibition of constitutive $I_{K,ACh}$ channels with the highly selective $I_{K,ACh}$-blocker tertiapin reverses the APD abbreviation and AF promotion in dogs with ATR (Cha *et al.*, 2006). Since $I_{K,ACh}$ is absent in ventricles, constitutively active $I_{K,ACh}$ is considered as a promising atrial-selective anti-AF target, without proarrhythmic side effects in the ventricles (Dobrev and Nattel, 2010).

Here, we describe the voltage-clamp techniques that can be used to study constitutive $I_{K,ACh}$ activity in atrial myocytes and we summarize briefly the current knowledge about the potential underlying mechanism of constitutive $I_{K,ACh}$ activity in diseased heart.

2. Recording of Constitutive $I_{K,ACh}$ Using Patch-Clamp Techniques

2.1. Basic principles of patch-clamp technique

The development of the patch-clamp technique was based on the ambition to record currents through individual ion channels in intact cells. Erwin Neher and Bert Sakmann developed the patch-clamp technique in the late 1970s and early 1980s (Hamill *et al.*, 1981; Neher and Sakmann, 1976; Sigworth and Neher, 1980). The major breakthrough was the discovery that application of slight suction within a freshly prepared glass pipette used as an electrode (Fig. 32.1) results in formation of very high seal resistances (up to several giga-ohms) between the pipette and the cellular membrane (giga-seal). The giga-seal formation reduces the electrical background noise and enables to measure ion

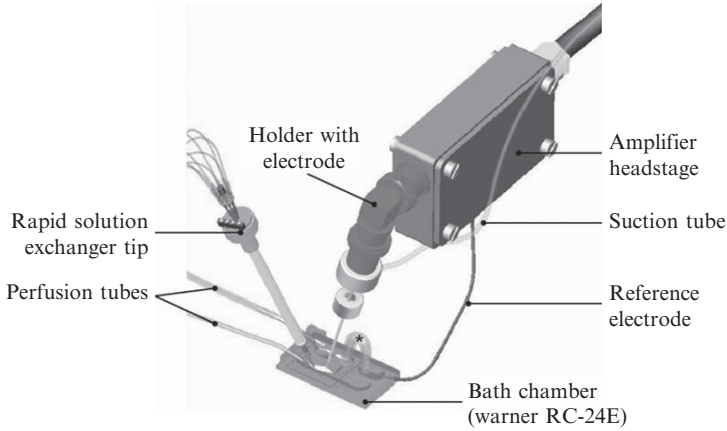

Figure 32.1 **Bath chamber with associated devices for electrophysiological measurements, bath perfusion, and rapid solution exchange. The reference electrode is connected to the bath solution via an agar bridge (*), allowing separation of bath and reference electrode solution.**

currents through single channels in a pA range (cell-attached configuration, Fig. 32.2A). Furthermore, it was recognized that giga-seal formation provides mechanical stability, so that the membrane patch can be excised from the intact cell (cell-free inside-out (I-O) configuration, Fig. 32.2A). However, breaking the patch by suction on the pipette provides electrical continuity between the patch pipette and the cell interior (whole-cell configuration, Fig. 32.2A), similar to conventional microelectrode recordings. Here, we do not discuss other advanced configurations like outside-out or perforated-patch and refer the interested readers to excellent descriptions of these techniques in previous issues of this book (Cahalan and Neher, 1992).

The application of correct voltages is challenging because depending on the patch-clamp configuration used (Fig. 32.2B) the potential applied through the pipette (E_P) may differ substantially from the potential "seen" by the patch membrane (V_C). In the cell-attached configuration, the potential across the membrane patch (V_C) equals the membrane potential of the cell (E_M) minus the pipette potential (E_P). Since the pipette potential applied by the patch-clamp amplifier (E_P) indicates the potential of the patch electrode with reference to the bath electrode (reference electrode; Fig. 32.1), the pipette potential (E_P) equals the membrane potential ($E_P = E_M = V_C$) only in whole-cell configuration, where the pipette is connected to the interior of the cell. In the case of I-O configuration, the electrodes are reversed with the patch pipette facing the exterior and the bath solution facing the interior of the membrane patch. Therefore, the potential across the membrane patch equals the reverse potential of the pipette ($V_C = -E_P$).

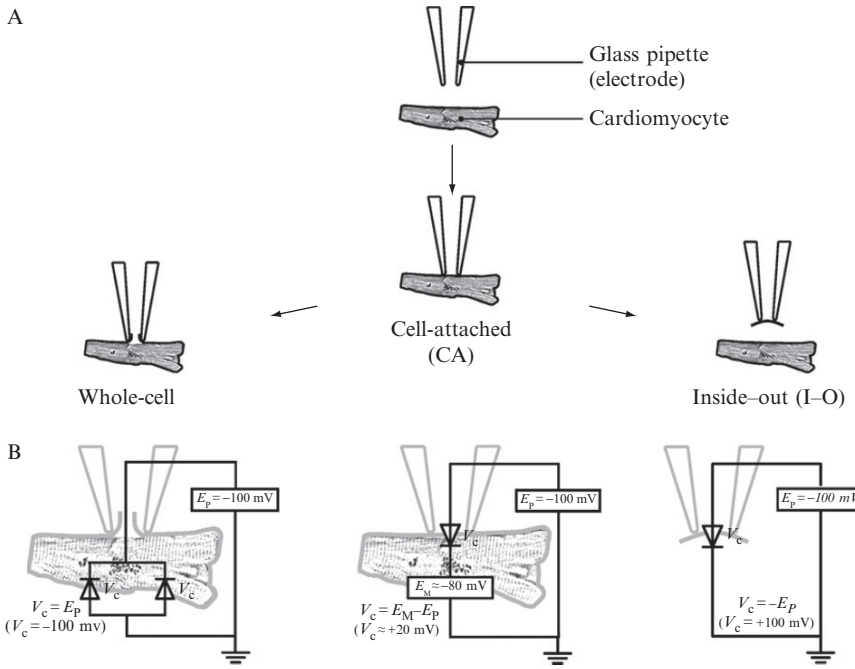

Figure 32.2 Different patch-clamp configurations that can be used to study $I_{K,ACh}$ (A) and corresponding considerations for voltage application (B). Depending on the configuration, the voltage seen by the studied ion channel (V_C) is set by variation of the pipette potential (E_P), which indicates the potential of the patch electrode with reference to the bath electrode (reference electrode, see Fig. 32.1). In inside-out configuration, V_C is also influenced by the membrane potential (E_M), which depends largely on the potassium concentration in the bath solution. See text for further details.

2.2. Isolation of human atrial cardiomyocytes

Studying electrophysiological properties of cardiac ion channels with the patch-clamp technique requires isolated single myocytes, which are usually obtained following the *in vitro* exposure of cardiac tissue samples to digestive enzymes (collagenase, hyaluronidase, peptidase, etc.). Since the first report of isolation of viable cardiac myocytes in 1955 (Margaret, 1955), a large quantity of protocols have been developed in order to harvest single atrial and ventricular myocytes from different species including mouse, rat, rabbit, dog, guinea pig, and human. Here, we describe in detail the isolation of human atrial cardiomyocytes, which generally derives from the procedure described by Bustamante *et al.* (1982). Regarding procedures used for isolation of atrial myocytes from other species, we refer to the "Worthington Tissue Dissociation Guide" provided by Worthington Biochemical Corp., USA (www.tissuedissociation.com).

During routine cannulation procedures in patients undergoing open-heart surgery for cardiopulmonary bypass grafting, the tip of the right atrial appendage is usually removed and can be used for isolation of atrial cardiomyocytes. After excision, the tissue sample is transferred immediately into sterile 2,3-butanedione monoxime (contractile inhibitor, preventing myocyte contracture) containing Ca^{2+}-free solution for transportation (see Table 32.1). At a general transport time of about 30 min, we did not recognize a clear advantage of cooling with respect to both number and quality of isolated atrial cardiomyocytes.

After removal of fat and connective tissue, the myocardial tissue, usually between 200 and 400 mg, is transferred to Ca^{2+}-free solution (without 2,3-butanedione monoxime; Table 32.1) and chopped into small chunks of $\sim 1\ mm^3$ in size. The following steps should be executed at 37 °C and under continuous gassing with 100% O_2. Primarily the tissue chunks are washed three times for 3 min in Ca^{2+}-free solution. For the first digestive step, the tissue is stirred for 45 min in 20 ml Ca^{2+}-free solution containing collagenase I and protease XXIV (enzyme solution E1; Table 32.1) with $[Ca^{2+}]$ being raised to 0.02 m*M* (add 40 µl of 10 m*M* stock solution) after 10 min. The enzyme solution is then exchanged for 20 ml enzyme solution E2 (Table 32.1) containing collagenase I only and stirring is continued until rod-shaped, striated cells appear. Due to the high variability among tissue samples from different donors, the duration of the second enzyme exposure varies between 5 and 45 min. After settling down of the tissue chunks, the supernatant is replaced by 20 ml of storage solution (Table 32.1; Feng *et al.*, 1998) and dissociation of the cells is achieved by gentle mechanical trituration using a Pasteur pipette. After separation from the debris by filtration through nylon gauze (200 µm mesh) and centrifugation for 10 min at $95 \times g$, the precipitate was redissolved in 4 ml of storage solution. The final Ca^{2+} concentration is set stepwise to 0.5 m*M* by adding a total amount of 0.2 ml 10 m*M* $CaCl_2$ within 20 min (80–40–80 µl). Usually, we obtain around 50 cells/10 µl and 30 cells/10 µl in samples from sinus rhythm (SR) and cAF patients, respectively. However, human cells are often more difficult to isolate than animal cells and cell yield varies largely, depending on degree of tissue fibrosis, age and cardiac diseases of the donor. The isolated atrial cardiomyocytes are kept at room temperature until use and should be used within 8 h.

2.3. Single-channel recordings of $I_{K,ACh}$ in cell-attached configuration

Since electrical properties of single-channel $I_{K,ACh}$ openings are clearly different compared to those of other ion channels (i.e., I_{K1}), single-channel registrations are suitable to provide direct evidence for increased constitutive $I_{K,ACh}$ activity in patients with cAF. Current amplitudes during

Table 32.1 Solutions for cell isolation

	Transport solution	Ca^{2+}-free solution	Enzyme solution E1	Enzyme solution E2	Storage solution
Albumin	–	–	–	–	1%
2,3-Butanedione monoxime	30	–	–	–	–
DL-β-Hydroxy-butyric acid	–	–	–	–	10
EGTA	–	–	–	–	10
Glucose	20	20	20	20	10
Glutamic acid	–	–	–	–	70
KCl	10	10	10	10	20
KH_2PO_4	1.2	1.2	1.2	1.2	10
$MgSO_4$	5	5	5	5	–
MOPS	5	5	5	5	–
NaCl	100	100	100	100	–
Taurin	50	50	50	50	10
Collagenase I (Worthington)	–	–	286 U/ml	286 U/ml	–
Protease XXIV	–	–	5 U/ml	–	–
pH	7.0	7.0	7.0	7.0	7.4
Adjusted with	1 *M* NaOH	1 *M* NaOH	1 *M* NaOH	1 *M* NaOH	1 *M* KOH

Concentrations in m*M* unless otherwise stated. All drugs were from Sigma-Aldrich (USA) unless otherwise stated.

single-channel measurements are lower (pA range) compared to whole-cell recordings (nA range) and therefore require higher efforts on reduction of electrical noise to improve the signal-to-noise ratio. Here we will describe briefly some steps that we found critical to reduce electrical noise and improve quality of single-channel recordings.

The first important step is to remove all electrical devices except the preamplifier from the Faraday cage including the light source of the microscope, which should be exchanged with a cold light source positioned outside the cage. We use a gravity-driven perfusion system to apply fresh bath solution (Table 32.2). The Faraday cage should be closed on all sides during the experiment. Furthermore, high efforts should be spend on pipette fabrication. We use sylgard (World Precision Instruments, USA)-coated pipettes fabricated from borosilicate glass capillaries (1.5 mm outer diameter, 0.87 mm inner diameter, 0.2 mm filament, Hilgenberg, Germany). Since the pipette acts as a capacitator with a capacitance proportional to 1/wall thickness, thereby causing electrical noise, coating of the pipette with a thick nonconducting layer reduces electrical noise. In addition, the hydrophobic nature of sylgard prevents the bath solution from creeping up the sides of the pipette, thereby reducing electrical contact between pipette and bath solution. Sylgard should be applied as near to the pipette tip as possible (10–50 μm) and extend until the pipette shoulder. It is cured by placing the pipette tip into a heated wire coil for a few seconds. After

Table 32.2 Bath solutions

	CA and whole-cell experiments	I-O experiments (phosphatases intact)	I-O experiments (phosphatases inhibited)
$CaCl_2$	2	–	–
EGTA	–	0.1	0.1
Glucose	10	–	–
HEPES	10	5	5
KCl	20	145	145
$MgCl_2$	1	1	1
NaCl	120	20	–
NaF	–	–	1
Na_3VO_4	–	–	0.1
$Na_2P_2O_7$	–	–	10
$ZnSO_4$	–	–	5
pH	7.4	7.4	7.4
Adjusted with	1 *M* NaOH	1 *M* Tris-acetat	1 *M* Tris-acetat

Concentrations in m*M*; CA, cell-attached configuration; I-O, inside-out configuration. All drugs were from Sigma-Aldrich (USA) unless otherwise stated.

Table 32.3 Pipette filling solutions

	CA and I-O experiments	Whole-cell experiments
$CaCl_2$	2	2
DL-Aspartic acid K^+ salt	–	80
EGTA	–	5
GTP-Tris	–	0.1
HEPES	5	10
KCl	145	40
Mg-ATP	–	5
$MgCl_2$	1	–
NaCl	–	8
pH	7.4	7.4
Adjusted with	1 *M* KOH	1 *M* KOH

Concentrations in m*M*; CA, cell-attached configuration; I-O, inside-out configuration. All drugs were from Sigma-Aldrich (USA) unless otherwise stated.

coating, pipettes should be fire polished using a microforge to clean and smooth the tip. Finally, pipettes should be cut to 2 cm total length. Because of the high $I_{K,ACh}$ channel density, pipettes should be relatively small, with tip resistances being ~8–10 MΩ when filled with pipette solution (Table 32.3, CA Experiments). Small-tip pipettes increase the likelihood of having only one channel within the patch, which allows a much more reliable analysis of single-channel properties (see below).

Figure 32.3A shows representative recordings of $I_{K,ACh}$ in the absence and presence of an M-receptor agonist in atrial myocytes from patients with sinus rhythm (SR) and cAF. Constitutive $I_{K,ACh}$ activity was quite apparent in cAF, whereas it occurred only sporadically in myocytes from patients with SR. Inclusion of the nonselective M-receptor agonist carbachol (CCh, 10 μ*M*) in the pipette solution strongly activated $I_{K,ACh}$ in both SR and cAF, causing frequent channel openings.

A detailed description of the single-channel analysis algorithms is clearly beyond the scope of this chapter. For more details regarding analysis of single-channel properties, see Colquhoun (1994), http://www.utdallas.edu/~tres/microelectrode/me.html. An elementary property characterizing single-channel activity is the sojourn time at the open and closed level. To characterize closed and open times, transitions between the two current levels must be detected. We usually use the threshold-crossing method, which automatically detects transitions from the closed to the open state or vice versa every time the observed current crosses the 50% threshold (idealization). The opening times obtained in this way can be displayed in an open-time histogram as shown in Fig 32.3B and open-time constants (τ_{open}) can be calculated by mono-exponential fits. Open-time constants

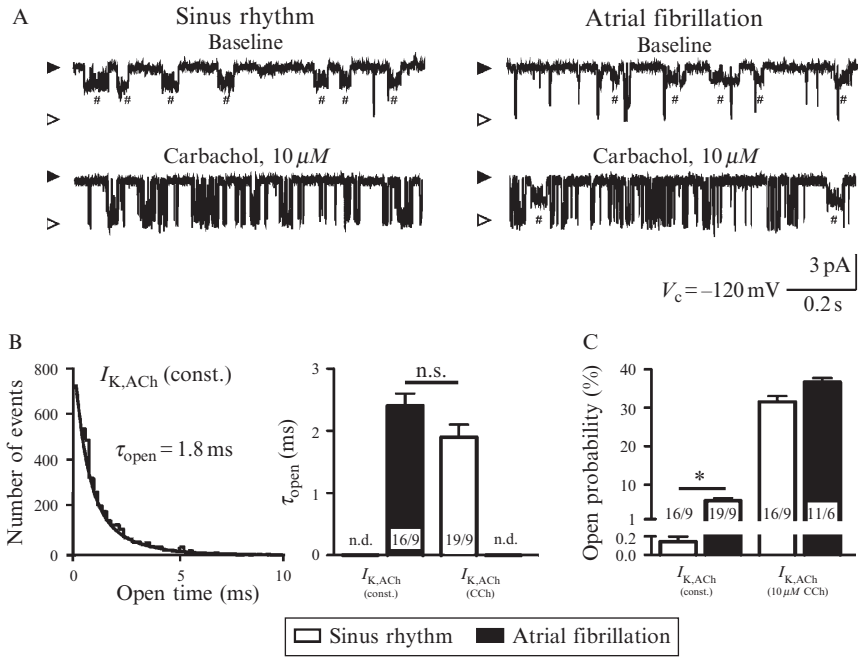

Figure 32.3 Single-channel properties of constitutively active $I_{K,ACh}$ channels in atrial myocytes from patients with chronic atrial fibrillation (cAF). (A) Representative cell-attached single-channel recordings of I_{K1}, constitutively active and cabachol (CCh)-activated $I_{K,ACh}$ in myocytes from sinus rhythm (SR, left) and cAF patients (right). Closed and open levels are indicated by filled and empty arrowheads, respectively. In the absence of M-receptor agonists (baseline), myocytes from the cAF patients exhibit both I_{K1} (#) and constitutive $I_{K,ACh}$ openings (*), whereas the latter is a rare event in myocytes from SR patients. (B) Representative histogram of open times of the constitutively active $I_{K,ACh}$ channel (left). Bin-width was 0.2 ms. Open-time constants were calculated for CCh-activated $I_{K,ACh}$ in SR patients and constitutively active $I_{K,ACh}$ in cAF patients by monoexponential fits and are expressed as mean ± S.E.M. (right). n.d., not determined. (C) Channel open probability of constitutively active and CCh-activated $I_{K,ACh}$ channels are expressed as mean ± S.E.M. $^*P < 0.05$. (B, C) Numbers within the columns indicate number of myocytes/patients. (Reprinted with permission from Dobrev *et al.*, 2005.)

from constitutive $I_{K,ACh}$ channels are comparable to $I_{K,ACh}$ channels activated with CCh, providing strong evidence for the identity of these spontaneous current openings as $I_{K,ACh}$. Since density of $I_{K,ACh}$ channels in atrial cardiomyocytes is high, patch membranes usually contain two or more channels under the patch pipette, indicated by two or more opening levels caused by simultaneous channel openings. However, since reliable determination of closed-time duration can only be performed with one channel in the patch, we usually refrain from analyzing closed times.

An additional parameter that can be obtained after calculation of open-time durations is the probability of a channel to open (open probability, P_{open}). P_{open} can be estimated by the total open time divided by the total length of the record. Again, a reliable estimate of P_{open} can be obtained only in the presence of only one individual $I_{K,ACh}$ channel in the membrane patch. Since presence of only one channel is a rare event precluding a reliable determination of the exact number of channels in the membrane patch, open probability is often expressed as nPo, where n indicates the usually unknown number of channels. Figure 32.3C shows higher nPo of constitutive $I_{K,ACh}$ in myocytes from patients with cAF compared to SR. Inclusion of the M-receptor agonist CCh further increases nPo without significant differences between cAF and SR.

The analysis of single-channel amplitudes in relation to the applied voltage (V_C) provides a further evidence for the identity of the studied channel (Fig 32.4A). To calculate $I_{K,ACh}$ amplitude, we generate point amplitude histograms by plotting all digitized current events according to their individual current values in a histogram (Fig. 32.4B). There is usually one peak at the

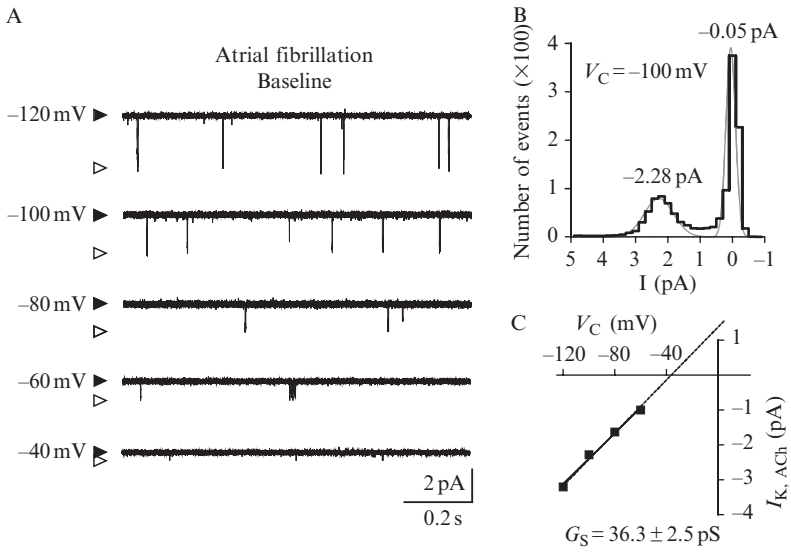

Figure 32.4 Single-channel conductance of constitutively active $I_{K,ACh}$ channels in a myocyte from one patient with chronic atrial fibrillation. (A) Representative single-channel recordings at various potentials (V_C; see Fig. 32.2). Closed and open levels are indicated by filled and empty arrowheads, respectively. (B) Corresponding amplitude histogram at −100 mV. Bin-width was 0.2 pA. After fitting two Gaussian distribution curves, single-channel $I_{K,ACh}$ amplitude equals the difference between the two peaks at −0.05 pA (closed level) and −2.28 pA (open level). (C) Current–voltage relation calculated from the corresponding amplitude histograms.

closed level and one peak at the open level. The single-channel $I_{K,ACh}$ amplitude equals the difference between both peaks. Since again any drift in baseline will bias the results, an appropriate baseline correction should be performed in advance. In addition, single-channel openings of constitutive $I_{K,ACh}$ are relatively rare; therefore, we recommend to confine the histogram to those points that correspond to periods when the channel is open. Plotting the amplitude values against the corresponding voltage applied on the patch (V_C) results in an almost linear relationship with the slope representing the single-channel conductance (Fig. 32.4C). The conductance obtained in atrial myocytes from cAF patients in absence of an M-receptor agonist (36.3 pS) is comparable to published values of agonist-activated $I_{K,ACh}$ and is clearly different from typical single-channel conductances of other inward-rectifier potassium currents like I_{K1} and ATP-dependent K^+ currents ($I_{K,ATP}$) (Heidbuchel *et al.*, 1990b).

2.4. Whole-cell recording of constitutive $I_{K,ACh}$

Whereas single-channel measurements are valuable for the direct proof of constitutive $I_{K,ACh}$ activity, they are not feasible to evaluate the relative contribution of constitutive $I_{K,ACh}$ activity to total inward-rectifier K^+ current. In addition, in whole-cell configuration, the channels are not shielded by the patch pipette and the applied drugs reach the channel quickly without any access restrictions, which allows a reliable testing of drug effects on channel function (Kitamura *et al.*, 2000). In whole-cell configuration, direct electrical access to the cell interior is obtained by disrupting the patch membrane after giga-seal formation. Successful disruption, achieved by applying gentle suction to the pipette, is indicated by the occurrence of capacitance artifacts in response to a distinct voltage step in the mV range. Since these capacitance artifacts are mainly due to cell membrane recharges, they are usually used for estimation of the cardiomyocyte surface area, assuming a membrane capacitance per unit area of about 1 $\mu F/cm^2$ (Gentet *et al.*, 2000).

In whole-cell configuration, the patch-pipette filling solution is in direct contact with the cytosol and should therefore have a similar ion concentration (Table 32.3). Borosilicate glass microelectrodes (1.5 mm outer diameter, 0.87 mm inner diameter, 0.2 mm filament, Hilgenberg, Germany) with tip resistances of 2–5 MΩ are acceptable. The myocytes are superfused with bath solution (Table 32.2). We use high (20 m*M*) extracellular potassium concentration because this shifts the reversal potential to more positive values and allows to record much larger (more easily measurable/comparable) inwardly directed K^+ currents (Dobrev *et al.*, 2000, 2001, 2005; Himmel *et al.*, 2000; Voigt *et al.*, 2007). We recorded the currents at room temperature because current amplitudes at room temperature are comparable to those at 37 °C and the success rate of experiments is much

higher at room temperature (Voigt *et al.*, 2010b), especially when using human atrial myocytes.

Drugs are generally applied via a rapid solution-exchange-system (ALA-Scientific-Instruments, USA). Agonist-inducible $I_{K,ACh}$ is stimulated with CCh (2 μM) and defined as the difference current between total current in the presence of CCh and basal current. Basal inward-rectifier currents and $I_{K,ACh}$ are specifically assessed as Ba^{2+}(1 mM)-sensitive currents. Since both I_{K1} and constitutive $I_{K,ACh}$ channels contribute to basal inward-rectifier K^+ current in atrial myocytes, the whole-cell configuration is not feasible for direct detection of constitutive $I_{K,ACh}$. However, selective $I_{K,ACh}$-channel blockers and specific voltage protocols targeting differences in time-dependent $I_{K,ACh}$ "relaxation" allow sufficient differentiation between constitutive $I_{K,ACh}$ currents and I_{K1} also in the whole-cell voltage-clamp configuration.

2.4.1. Use of selective $I_{K,ACh}$-channel blockers

Drugs like NIP-142, NIP-151, and AVE0118 are shown to block $I_{K,ACh}$ in atrial myocytes; however, their selectivity for $I_{K,ACh}$ is imperfect (Christ *et al.*, 2008; Hashimoto *et al.*, 2008; Tanaka and Hashimoto, 2007). In addition, inhibition of constitutively active $I_{K,ACh}$ may contribute to the efficacy of commonly used class I and III antiarrhythmic drugs (Voigt *et al.*, 2010a). Tertiapin, a 21-amino acid containing peptide initially isolated from the venom of the European honey bee, has been characterized as a selective blocker of Kir3.1 and Kir3.4 heteromultimers, renally expressed Kir1.1a (ROMK1) channels and Ca^{2+}-dependent large-conductance K^+ channels (BK channels) in a nanomolar range (Jin and Lu, 1998; Kanjhan *et al.*, 2005). Kir1.1b (ROMK2) and Kir2.1 (Jin and Lu, 1998) channels are inhibited in the micromolar range only (Jin and Lu, 1998; Sackin *et al.*, 2003). Since ROMK channels are not expressed in cardiac myocytes and inhibition of BK channels occurs only after myocyte incubation for at least 15 min (Kanjhan *et al.*, 2005), acute application of tertiapin in atrial myocytes can be considered as highly selective for $I_{K,ACh}$ inhibition. It is suggested that tertiapin blocks $I_{K,ACh}$ channels by interaction of its α-subunit C-terminus with the external side of the channel pore (Jin *et al.*, 1999). This interaction with the extracellular side of the channel may explain the delayed inhibitory effect of tertiapin in cell-attached configuration, where the channel is largely isolated from the bath solution by the patch-pipette (Voigt *et al.*, 2008). For experimental purposes, we recommend the usage of a non-air-oxidizable derivate, called tertiapin-Q, in which the methionine residue 13 is replaced by glutamine (Jin and Lu, 1999). Tertiapin-Q functionally resembles native tertiapin in both affinity and specificity, but is much more stable. On experimental days, we prepare fresh working solutions of tertiapin (0.1–100 nM) using a 100-μM stock

solution stored at −15 °C. In addition, 1 mg/ml albumin should be added to the bath solution to reduce nonspecific protein binding of tertiapin.

At the whole-cell configuration, we activate the inward-rectifier currents using a ramp pulse from −100 to +40 mV (Fig 32.5A), which is much better tolerated by human atrial myocytes compared to clamp steps. A direct comparison between results obtained with ramp pulses versus clamp steps indicated their similarity and supported the validity of results obtained with ramp-pulse protocols (Voigt *et al.*, 2010b). Figure 32.5B shows the time course of inward-rectifier current at −100 mV. Application of the M-receptor agonist CCh (2 μ*M*) resulted in a rapid initial current increase (Peak), followed by a decrease to a quasi-steady state level (QSS). The agonist-dependent $I_{K,ACh}$ currents at Peak and QSS level are defined as CCh-sensitive current increases (Peak- and QSS-$I_{K,ACh}$). In the absence of M-receptor agonists, application of the highly selective $I_{K,ACh}$-blocker tertiapin (0.1–100 n*M*) to myocytes from SR patients resulted only in a slight reduction of basal inward-rectifier K^+ current, which was comparable to values in control experiments with application of bath solution only. In contrast, tertiapin reduced basal current in cAF patients in a concentration-dependent manner (Fig. 32.5C). In addition, tertiapin inhibited the CCh-mediated activation of $I_{K,ACh}$ in both SR and cAF, confirming the potency and efficacy of tertiapin as a selective $I_{K,ACh}$-channel blocker (Fig. 32.5D). Taken together, these data suggest the existence of substantial constitutive $I_{K,ACh}$ activity in cAF only.

2.4.2. Estimation of time-dependent $I_{K,ACh}$ "relaxation"

Apart from the use of selective $I_{K,ACh}$ blockers, differences in electrophysiological properties can be also utilized to differentiate I_{K1} and constitutive $I_{K,ACh}$ currents in whole-cell patch-clamp experiments. An elegant method is the analysis of activation kinetics upon a hyperpolarizing voltage step pulse. Whereas an instantaneous increase of current amplitude upon hyperpolarization is characteristic for almost all inward-rectifier K^+ currents, the time-dependent current increase, called "relaxation," is a hallmark of $I_{K,ACh}$ currents only (Hibino *et al.*, 2010). Although the exact mechanism is largely unknown, regulators of G protein signaling (RGS-proteins), which accelerate GTPase activity of the Gα-subunit, appear essential for reconstituting the relaxation behavior of $I_{K,ACh}$ current in Xenopous oocytes expressing Kir3.1/Kir3.4 channels together with M_2 receptors (Fujita *et al.*, 2000). As shown in Fig. 32.6, Cha *et al.* used this phenomenon to demonstrate increased time-dependent hyperpolarization-activated inward-rectifier current (I_{KH}) in atrial myocytes from dogs with ATR (Cha *et al.*, 2006). I_{KH} is inhibited by tertiapin-Q, and single-channel recordings in atrial myocytes from dogs with ATR directly confirmed the identity of I_{KH} as constitutive $I_{K,ACh}$ (Voigt *et al.*, 2008).

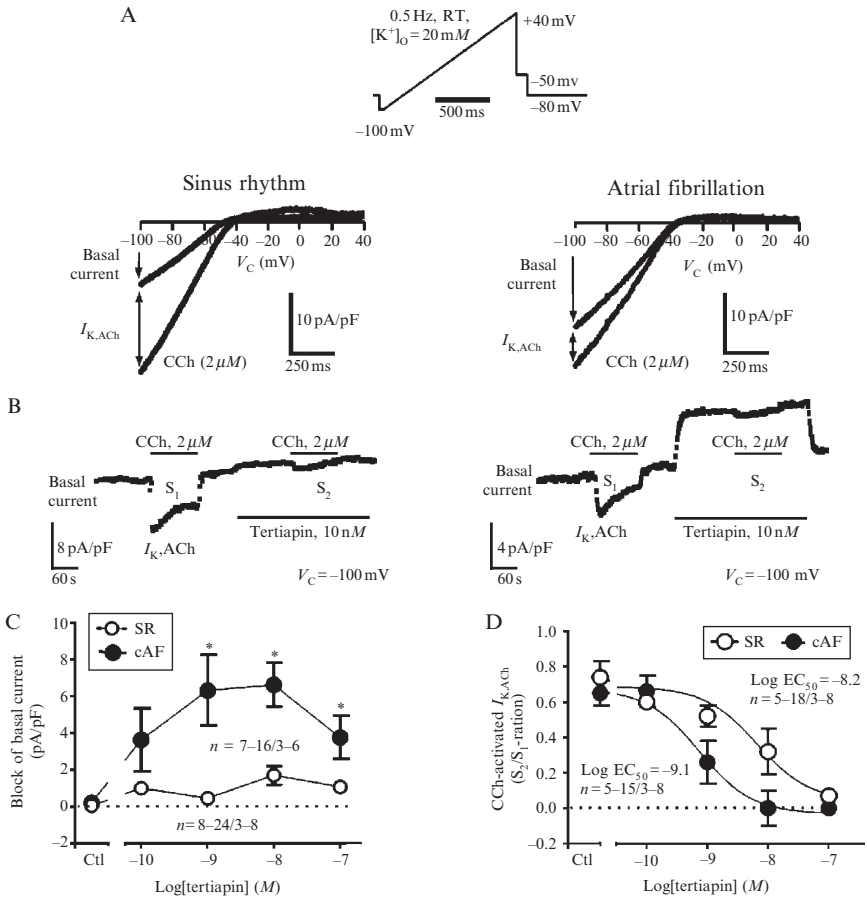

Figure 32.5 Detection of constitutive $I_{K,ACh}$ activity in whole-cell configuration with the highly selective $I_{K,ACh}$-blocker tertiapin. (A) Representative inward-rectifier current recordings under basal conditions (basal current) and in response to 2 μ*M* carbachol (CCh) in myocytes from a patient with sinus rhythm (SR, left) and chronic atrial fibrillation (cAF, right), respectively. Top: Ramp protocol. (B) Corresponding time course of basal inward-rectifier current and CCh-activated $I_{K,ACh}$ at −100 mV. Tertiapin (10 n*M*) was applied before, during and after a second CCh application (S_2) with the first CCh application (S_1) serving as internal control. (C) Concentration-dependent block of basal current with tertiapin in SR and cAF patients unmasks increased constitutively active $I_{K,ACh}$ channels in cAF patients only. $^{\star}P < 0.05$ versus corresponding values in SR. (D) Concentration-dependent effects of tertiapin on the S_2/S_1 ratio of $I_{K,ACh}$. (C, D) Each point represents values (mean ± S.E.M., at −100 mV) from *n* independent experiments. Numbers within the figures indicate number of myocytes/patients. (Reprinted with permission from Dobrev *et al.*, 2005.)

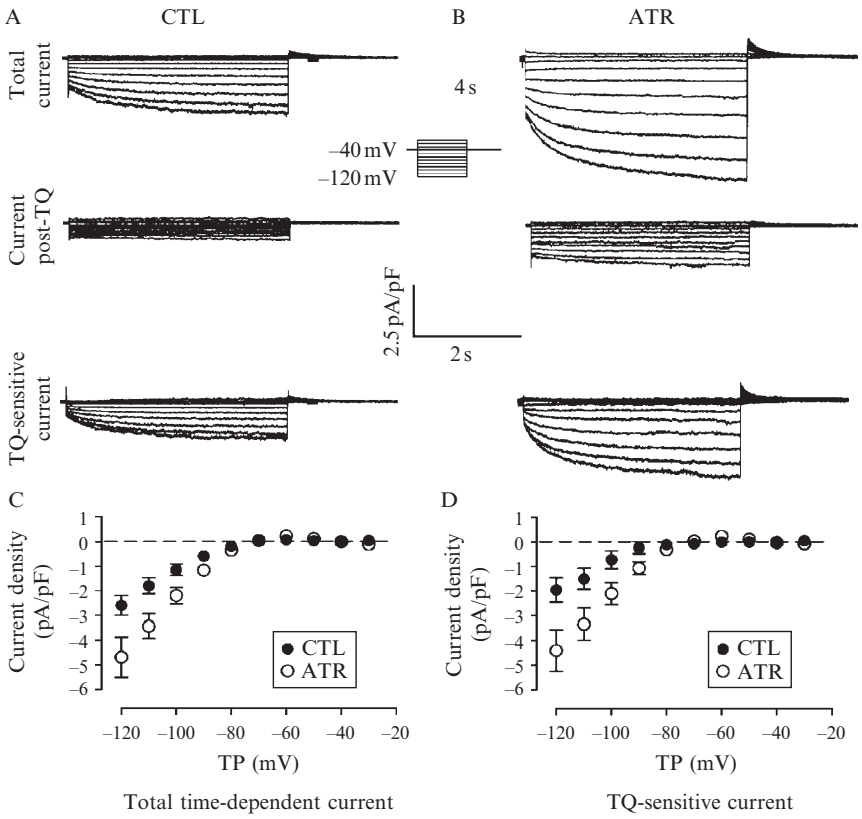

Figure 32.6 Estimation of constitutive $I_{K,ACh}$ activity in whole-cell configuration with a voltage-step protocol in canine atrial myocytes. (A and B, top) Representative current recordings in response to hyperpolarizing voltage steps (inset) in atrial myocytes from control (CTL) and atrial tachycardia-remodeled dogs (ATR). Middle: Currents from the same cells as in top panel in the presence of 100 n*M* tertiapin-Q, which selectively suppresses $I_{K,ACh}$, leaving essentially only I_{K1}. Bottom: Tertiapin-sensitive currents obtained in cells illustrated above by subtracting currents in presence of 100 n*M* tertiapin-Q from currents before superfusion. (C) Mean ± S.E.M. of constitutively active $I_{K,ACh}$ current density–voltage relations based on time-dependent activating current based on 18 cells from nine dogs (CTL) and 10 cells from four dogs (ATR), respectively. Currents in ATR dog cells were significantly greater than in CTL cells ($P = 0.02$). (D) Mean ± S.E.M. of constitutive $I_{K,ACh}$ density–voltage relations based on tertiapin-sensitive current densities based on nine cells from six dogs (CTL) and eight cells from three dogs (ATR), respectively. Currents in ATR dog cells were significantly greater than in CTL cells ($P = 0.02$). (C, D) TP indicates test potential. (Reprinted with permission from Cha *et al.*, 2006.)

2.5. Identification of the underlying mechanism(s) of constitutive $I_{K,ACh}$

Previous studies showed that the M-receptor antagonist atropine does not abolish the constitutive $I_{K,ACh}$ activity, suggesting that an agonist-independent mechanism might be implicated in the formation of constitutive $I_{K,ACh}$ channels (Dobrev *et al.*, 2005). An increased receptor-independent dissociation of G_{α}- and $G_{\beta\gamma}$-subunits appears unlikely contributor because neither pertussis toxin nor the absence of GTP affected the $I_{K,ACh}$-like component of basal whole-cell current in dog atrial myocytes (Ehrlich *et al.*, 2004). In addition, indirect evidence also suggests that upregulation and stronger membrane translocation of PKCε might cause hyperphosphorylation of $I_{K,ACh}$ channels in cAF patients, likely contributing to the increase in constitutive $I_{K,ACh}$ activity (Voigt *et al.*, 2007). Together, these findings point to a membrane-delimited phosphorylation-mediated mechanism of constitutive $I_{K,ACh}$.

In the I–O configuration, a small, cell-free piece of cell membrane containing the channel of interest is attached to the pipette with the cytosolic side facing the bath solution. This configuration allows direct alterations of the intracellular milieu which makes it particularly suitable for the exploration of the intracellular mechanism of constitutive $I_{K,ACh}$ activity. Here we describe how we use this method to study increased constitutive $I_{K,ACh}$ activity in dogs with ATR (Makary *et al.*, unpublished). For excision of the membrane patch, it is necessary that the myocytes are properly attached to the glass bottom of the chamber. Therefore, it is essential to allow enough time (~30 min) for myocytes to settle down before starting an experiment. Coating of the glass bottom with laminin may also improve the adhesion of the cells, but we did not find an advantage of using laminin coating. I-O patches are made based on the cell-attached configuration (see above). Very slow elevation of the pipette under continuous monitoring of single-channel activity should result in excision of the membrane patch out of the intact cell while preserving the giga-seal. Pulling off a membrane patch often results initially in the formation of a membrane vesicle in the pipette tip indicated by disappearance of the channel openings at preserved seal resistance. In order to reduce the chance of vesicle formation, we use pipettes with low seal resistance around 2–3 MΩ. If vesicle formation should still be a problem, the outer face of the vesicle can be opened by briefly taking the membrane through the bath solution/air interface, by positioning the tip in front of the outflow of the bath perfusion or by momentarily making contact with a droplet of paraffin or a piece of cured sylgard. However, these mechanical procedures are always critical because they may spoil the intact giga-seal.

After I-O formation, the cytosolic side of the channel faces the bath solution which is exchanged to a high K^+ bath solution (Table 32.2) in order to represent intracellular conditions and avoid K^+ gradients across the

membrane patch. Furthermore, it has to be considered that after I-O formation the potential seen by the patch is directly controlled by the amplifier and that the influence of the membrane potential is eliminated ($E_P = +100$ mV results in $V_c = -100$ mV, see above and Fig. 32.2B). After excision of the patch and formation of the I-O configuration, the constitutive $I_{K,ACh}$ activity of ATR cardiomyocytes is strongly reduced (Fig. 32.7A) and the resulting low opening probability becomes comparable to that of control cardiomyocytes, pointing to the contribution of a cytosolic factor to ATR-associated increase of constitutive $I_{K,ACh}$. Previous studies of agonist-activated $I_{K,ACh}$ revealed that inhibition of phosphatases is necessary to prevent run-down in cell-free I-O patches (Huang *et al.*, 1998; Kaibara *et al.*, 1991; Shui *et al.*, 1997), suggesting that normal $I_{K,ACh}$ activity requires channel phosphorylation (Heidbuchel *et al.*, 1990a; Medina *et al.*, 2000).

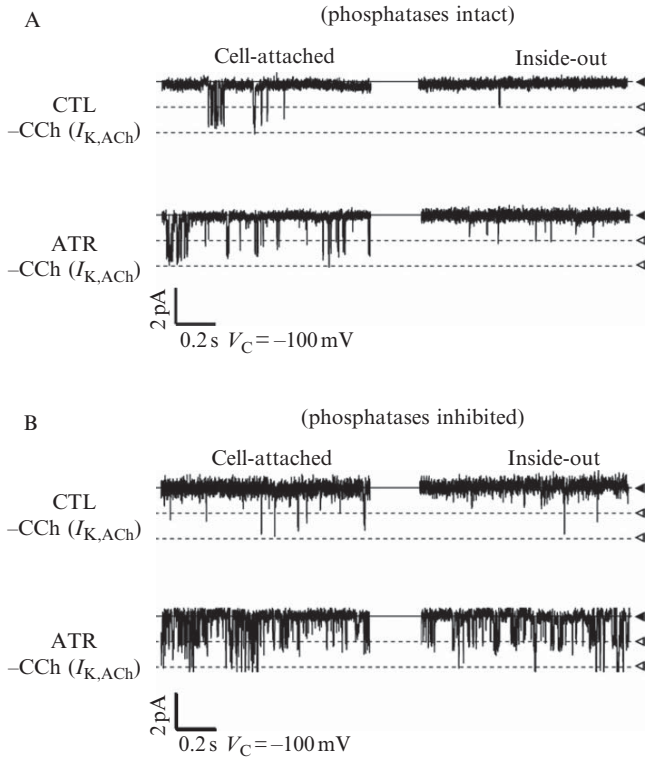

Figure 32.7 $I_{K,ACh}$ single-channel recordings in inside-out configuration. (A, B) Representative cell-attached (left) and inside-out (right) recordings of constitutively active $I_{K,ACh}$ in the absence (A) and presence (B) of protein phosphatase inhibitors. Closed and open levels are indicated by filled and empty arrowheads, respectively (Makary *et al.*, unpublished observations).

To assess the contribution of channel phosphorylation to constitutive $I_{K,ACh}$ activity in ATR, we added phosphatase inhibitors (fluoride, vanadate, and pyrophosphate, Table 32.2) to the bath solution. Under these conditions, the open probability of constitutive $I_{K,ACh}$ channels in ATR cardiomyocytes was only slightly reduced after I-O formation (Fig. 32.7B) compared to cell-attached experiments and the differences between control and ATR were preserved. The results in Fig. 32.7 indicate a crucial role of phosphorylation in development of constitutive $I_{K,ACh}$ channel activity. These findings provide an example of how I-O recordings may be used to explore the molecular mechanisms of constitutive $I_{K,ACh}$. Further studies are necessary to elaborate whether and how specific phosphorylation processes contribute to the development of constitutive $I_{K,ACh}$ activity in cAF.

3. Conclusions and Perspective

Although impaired channel phosphorylation is a potential contributor to development of constitutive $I_{K,ACh}$ activity in cAF, the complex regulation of agonist-activated $I_{K,ACh}$ makes several underlying mechanisms possible (Fig. 32.8A). Physiological activation of $I_{K,ACh}$ requires binding of $G_{\beta\gamma}$-subunits to the $I_{K,ACh}$ channel, which strengthens the interaction between channel subunits and cell membrane-located phosphatidylinositol 4,5-bisphosphate (PIP_2; Huang *et al.*, 1998). It is known that depletion of PIP_2 and removal of ATP both prevent activation of $I_{K,ACh}$ by $G_{\beta\gamma}$-subunits, suggesting tonic channel phosphorylation and sufficient PIP_2 levels in the cell membrane as absolute requirements for $G_{\beta\gamma}$-mediated activation of $I_{K,ACh}$ (Medina *et al.*, 2000; Sui *et al.*, 1998). In contrast, enhanced channel phosphorylation and/or increased amount of PIP_2 close to the channel may activate the channel even in the absence of $G_{\beta\gamma}$-subunits (Kaibara *et al.*, 1991; Kim, 1993; Okabe *et al.*, 1991). In addition, Na^+ enhances the interaction of PIP_2 with the $I_{K,ACh}$ channel indicating that AF-associated Na^+-overload might also contribute to constitutive $I_{K,ACh}$ (Mark and Herlitze, 2000). As mentioned above, activation of $I_{K,ACh}$ requires ATP which may modulate the channel through multiple mechanisms: (i) direct phosphorylation of the channel and/or channel regulatory proteins (Kim, 1993; Medina *et al.*, 2000), (ii) generation of PIP_2 (Huang *et al.*, 1998), and (iii) transphosphorylation between adenosine and guanosine nucleosides via nucleoside diphosphate kinase (NDPK; Heidbuchel *et al.*, 1990a). In principle, each of these mechanisms may contribute to the development of cAF-associated constitutive $I_{K,ACh}$ activity. The here described patch-clamp techniques in combination with suitable biochemical and molecular biology methods (i.e., adenoviral transfection of cultured human atrial myocytes,

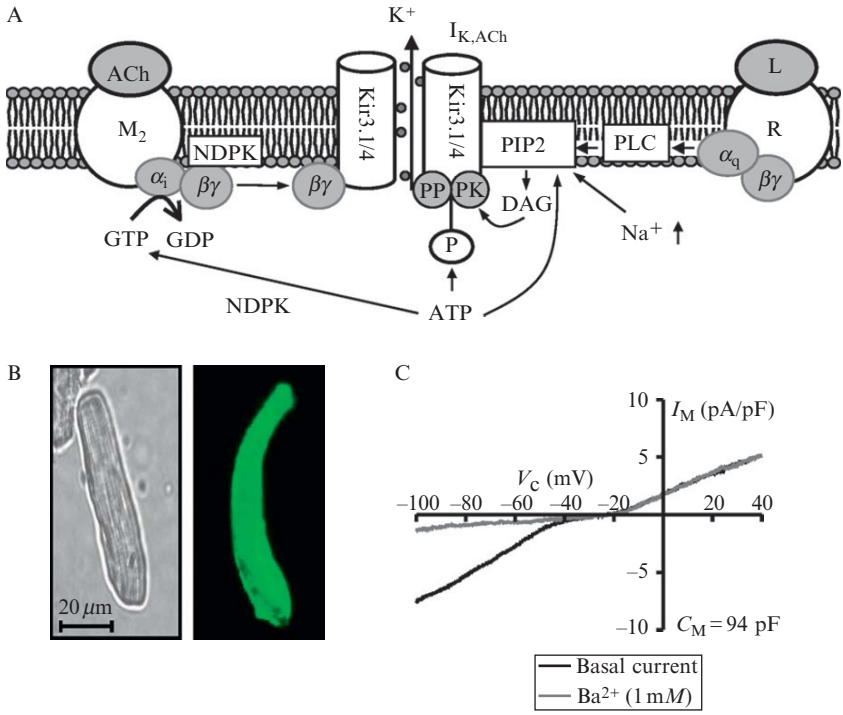

Figure 32.8 Regulatory mechanisms of $I_{K,ACh}$ in the atrium. (A) Binding of the vagal neurotransmitter acetylcholine (ACh) to muscarinic M_2 receptors leads to dissociation of G_i protein α- and βγ-subunits. In addition, transphosphorylation between adenosine and guanosine nucleosides via nucleoside diphosphate kinase (NDPK) may cause receptor-independent G_i protein dissociation. In both cases, the consecutive binding of G_i protein βγ-subunits to the $I_{K,ACh}$ channel subunits Kir3.1 and Kir3.4 strengthens their interaction with cell membrane-located phosphatidylinositol 4,5-bisphosphate (PIP_2), thereby increasing $I_{K,ACh}$ open probability. Similarly increased intracellular Na^+ also strengthens the interaction of PIP_2 with the channel leading to receptor-independent current activation. In contrast, stimulation of G_q-coupled receptors (R; i.e., AT_1-receptors or α_1-adrenoceptors) activates phospholipase-C (PLC), thereby lowering the PIP_2 membrane content, which results in $I_{K,ACh}$ inhibition. Furthermore, the PIP_2 metabolite diacylglycerol activates protein kinase C that phosphorylates $I_{K,ACh}$ channel subunits. In general, channel phosphorylation, which is dynamically regulated by protein kinases (PK) and phosphatases (PP), is an absolute requirement for normal $I_{K,ACh}$ function. Adenosine triphosphate (ATP) modulates the channel through multiple actions: (i) direct phosphorylation of the channel and/or channel regulatory proteins, (ii) generation of PIP_2, and (iii) transphosphorylation between adenosine and guanosine nucleosides via nucleoside diphosphate kinase (NDPK). (B) Adenoviral-mediated expression of "enhanced green fluorescence protein" and the Gβγ-scavenger transducin-α. With bright-field microscopy, adenovirally transfected human right atrial myocytes are indistinguishable from nontransfected cells (left), whereas the fluorescence emission light at an excitation wavelength of 488 nm indicates successful transfection (right). (C) Basal inward-rectifier current (I_M) in response to a ramp pulse from −100 to +40 mV (see also Fig. 32.5A) measured in a human right atrial myocyte transfected with transducin-α. Identity as inward-rectifier current was specifically assessed by application of Ba^{2+} (1 m*M*). C_M, cell capacity.

Fig. 32.8B) are powerful tools to discover the underlying mechanism(s) of constitutive $I_{K,ACh}$ activity in the diseased heart.

ACKNOWLEDGMENTS

The authors thank Dr Thomas Wieland, University of Heidelberg, for the kind provision of adenoviruses for atrial cardiomyocyte transfection.
The authors' research is supported by the Deutsche Forschungsgemeinschaft (Do769/1-1-3 to D. D.), the German Federal Ministry of Education and Research through the Atrial Fibrillation Competence Network (01Gi0204 to D. D.), the Canadian Institutes of Health Research (MOP44365 to S. N.), and the European–North American Atrial Fibrillation Research Alliance (ENAFRA) grant of Fondation Leducq (07CVD03 to D. D. and S. N.).

REFERENCES

Blanchet, C., and Luscher, C. (2002). Desensitization of mu-opioid receptor-evoked potassium currents: Initiation at the receptor, expression at the effector. *Proc. Natl. Acad. Sci. USA* **99,** 4674–4679.

Bustamante, J. O., *et al.* (1982). Isolation of single atrial and ventricular cells from the human heart. *Can. Med. Assoc. J.* **126,** 791–793.

Cahalan, M., and Neher, E. (1992). Patch clamp techniques: An overview. *Methods Enzymol.* **207,** 3–14.

Cha, T. J., *et al.* (2006). Kir3-based inward rectifier potassium current: Potential role in atrial tachycardia remodeling effects on atrial repolarization and arrhythmias. *Circulation* **113,** 1730–1737.

Christ, T., *et al.* (2008). Pathology-specific effects of the IKur/Ito/IK, ACh blocker AVE0118 on ion channels in human chronic atrial fibrillation. *Br. J. Pharmacol.* **154,** 1619–1630.

Colquhoun, D. (1994). Practical analysis of single channel records. *In* "Microelectrode Techniques. The Plymouth Workshop Handbook," (D. C. Ogden, ed.), pp. 101–139. The Company of Biologists, Cambridge, UK.

Dobrev, D. (2006). Electrical remodeling in atrial fibrillation. *Herz* **31,** 108–112, quiz 142–143.

Dobrev, D., and Nattel, S. (2010). New antiarrhythmic drugs for treatment of atrial fibrillation. *Lancet* **375,** 1212–1223.

Dobrev, D., *et al.* (2000). G-Protein beta(3)-subunit 825T allele is associated with enhanced human atrial inward rectifier potassium currents. *Circulation* **102,** 692–697.

Dobrev, D., *et al.* (2001). Molecular basis of downregulation of G-protein-coupled inward rectifying K(+) current (I(K, ACh) in chronic human atrial fibrillation: Decrease in GIRK4 mRNA correlates with reduced I(K, ACh) and muscarinic receptor-mediated shortening of action potentials. *Circulation* **104,** 2551–2557.

Dobrev, D., *et al.* (2005). The G protein-gated potassium current I(K, ACh) is constitutively active in patients with chronic atrial fibrillation. *Circulation* **112,** 3697–3706.

Ehrlich, J. R., *et al.* (2004). Characterization of a hyperpolarization-activated time-dependent potassium current in canine cardiomyocytes from pulmonary vein myocardial sleeves and left atrium. *J. Physiol.* **557,** 583–597.

Feng, J., *et al.* (1998). Ultrarapid delayed rectifier current inactivation in human atrial myocytes: Properties and consequences. *Am. J. Physiol.* **275,** H1717–H1725.

Fujita, S., *et al.* (2000). A regulator of G protein signalling (RGS) protein confers agonist-dependent relaxation gating to a G protein-gated K + channel. *J. Physiol.* **526**(Pt 2), 341–347.
Gentet, L. J., *et al.* (2000). Direct measurement of specific membrane capacitance in neurons. *Biophys. J.* **79,** 314–320.
Hamill, O. P., *et al.* (1981). Improved patch-clamp techniques for high-resolution current recording from cells and cell-free membrane patches. *Pflugers Arch.* **391,** 85–100.
Hashimoto, N., *et al.* (2008). Characterization of in vivo and in vitro electrophysiological and antiarrhythmic effects of a novel IKACh blocker, NIP-151: A comparison with an IKr-blocker dofetilide. *J. Cardiovasc. Pharmacol.* **51,** 162–169.
Heidbuchel, H., *et al.* (1990a). ATP-dependent activation of atrial muscarinic K + channels in the absence of agonist and G-nucleotides. *Pflugers Arch.* **416,** 213–215.
Heidbuchel, H., *et al.* (1990b). Three different potassium channels in human atrium. Contribution to the basal potassium conductance. *Circ. Res.* **66,** 1277–1286.
Hibino, H., *et al.* (2010). Inwardly rectifying potassium channels: Their structure, function, and physiological roles. *Physiol. Rev.* **90,** 291–366.
Himmel, H. M., *et al.* (2000). Evidence for Edg-3 receptor-mediated activation of I(K.ACh) by sphingosine-1-phosphate in human atrial cardiomyocytes. *Mol. Pharmacol.* **58,** 449–454.
Huang, C. L., *et al.* (1998). Direct activation of inward rectifier potassium channels by PIP2 and its stabilization by Gbetagamma. *Nature* **391,** 803–806.
Ito, H., *et al.* (1994). Background conductance attributable to spontaneous opening of muscarinic K + channels in rabbit sino-atrial node cells. *J. Physiol.* **476,** 55–68.
Jin, W., and Lu, Z. (1998). A novel high-affinity inhibitor for inward-rectifier K + channels. *Biochemistry* **37,** 13291–13299.
Jin, W., and Lu, Z. (1999). Synthesis of a stable form of tertiapin: A high-affinity inhibitor for inward-rectifier K + channels. *Biochemistry* **38,** 14286–14293.
Jin, W., *et al.* (1999). Mechanisms of inward-rectifier K + channel inhibition by tertiapin-Q. *Biochemistry* **38,** 14294–14301.
Kaibara, M., *et al.* (1991). Regulation of spontaneous opening of muscarinic K + channels in rabbit atrium. *J. Physiol.* **433,** 589–613.
Kanjhan, R., *et al.* (2005). Tertiapin-Q blocks recombinant and native large conductance K + channels in a use-dependent manner. *J. Pharmacol. Exp. Ther.* **314,** 1353–1361.
Kim, D. (1993). Mechanism of rapid desensitization of muscarinic K + current in adult rat and guinea pig atrial cells. *Circ. Res.* **73,** 89–97.
Kitamura, H., *et al.* (2000). Tertiapin potently and selectively blocks muscarinic K(+) channels in rabbit cardiac myocytes. *J. Pharmacol. Exp. Ther.* **293,** 196–205.
Kovoor, P., *et al.* (2001). Evaluation of the role of I(KACh) in atrial fibrillation using a mouse knockout model. *J. Am. Coll. Cardiol.* **37,** 2136–2143.
Krapivinsky, G., *et al.* (1995). The G-protein-gated atrial K + channel IKACh is a heteromultimer of two inwardly rectifying K(+)-channel proteins. *Nature* **374,** 135–141.
Kurachi, Y., *et al.* (1986). On the mechanism of activation of muscarinic K + channels by adenosine in isolated atrial cells: Involvement of GTP-binding proteins. *Pflugers Arch.* **407,** 264–274.
Liu, L., and Nattel, S. (1997). Differing sympathetic and vagal effects on atrial fibrillation in dogs: Role of refractoriness heterogeneity. *Am. J. Physiol.* **273,** H805–H816.
Loewi, O. (1921). Über humorale Übertragbarkei der Herznervenwirkung. *Pflügers Arch.* **189,** 239–242.
Luscher, C., *et al.* (1997). G protein-coupled inwardly rectifying K + channels (GIRKs) mediate postsynaptic but not presynaptic transmitter actions in hippocampal neurons. *Neuron* **19,** 687–695.
Margaret, W. C. (1955). Pulsation, migration and division in dissociated chick embryo heart cells in vitro. *J. Exp. Zool.* **128,** 573–589.

Mark, M. D., and Herlitze, S. (2000). G-protein mediated gating of inward-rectifier K + channels. *Eur. J. Biochem.* **267,** 5830–5836.
Medina, I., *et al.* (2000). A switch mechanism for G beta gamma activation of I(KACh). *J. Biol. Chem.* **275,** 29709–29716.
Nattel, S., *et al.* (2008). Atrial remodeling and atrial fibrillation: Mechanisms and implications. *Circ. Arrhythm. Electrophysiol.* **1,** 62–73.
Neher, E., and Sakmann, B. (1976). Single-channel currents recorded from membrane of denervated frog muscle fibres. *Nature* **260,** 799–802.
Noma, A., and Trautwein, W. (1978). Relaxation of the ACh-induced potassium current in the rabbit sinoatrial node cell. *Pflügers Arch.* **377,** 193–200.
Okabe, K., *et al.* (1991). The nature and origin of spontaneous noise in G protein-gated ion channels. *J. Gen. Physiol.* **97,** 1279–1293.
Sackin, H., *et al.* (2003). Permeant cations and blockers modulate pH gating of ROMK channels. *Biophys. J.* **84,** 910–921.
Sakmann, B., *et al.* (1983). Acetylcholine activation of single muscarinic K + channels in isolated pacemaker cells of the mammalian heart. *Nature* **303,** 250–253.
Shui, Z., *et al.* (1997). ATP-dependent desensitization of the muscarinic K + channel in rat atrial cells. *J. Physiol.* **505**(Pt 1), 77–93.
Sigworth, F. J., and Neher, E. (1980). Single Na + channel currents observed in cultured rat muscle cells. *Nature* **287,** 447–449.
Sui, J. L., *et al.* (1998). Activation of the atrial KACh channel by the betagamma subunits of G proteins or intracellular Na + ions depends on the presence of phosphatidylinositol phosphates. *Proc. Natl. Acad. Sci. USA* **95,** 1307–1312.
Tanaka, H., and Hashimoto, N. (2007). A multiple ion channel blocker, NIP-142, for the treatment of atrial fibrillation. *Cardiovasc. Drug Rev.* **25,** 342–356.
Voigt, N., *et al.* (2007). Differential phosphorylation-dependent regulation of constitutively active and muscarinic receptor-activated IK,ACh channels in patients with chronic atrial fibrillation. *Cardiovasc. Res.* **74,** 426–437.
Voigt, N., *et al.* (2008). Changes in I K,ACh single-channel activity with atrial tachycardia remodelling in canine atrial cardiomyocytes. *Cardiovasc. Res.* **77,** 35–43.
Voigt, N., *et al.* (2010a). Inhibition of IK, ACh current may contribute to clinical efficacy of class I and class III antiarrhythmic drugs in patients with atrial fibrillation. *Naunyn Schmiedebergs Arch. Pharmacol.* **381,** 251–259.
Voigt, N., *et al.* (2010b). Left-to-right atrial inward-rectifier potassium current gradient in patients with paroxysmal versus chronic atrial fibrillation. *Circ. Arrhythm. Electrophysiol.* doi: 10.1161/CIRCEP.110.954636.
Yamada, M., *et al.* (1998). G protein regulation of potassium ion channels. *Pharmacol. Rev.* **50,** 723–760.